Scheduled Sequential Compressed Spectrum Sensing for Wideband Cognitive Radios

Jie Zhao, *Student Member, IEEE*, Qiang Liu, *Member, IEEE*,
Xin Wang, *Member, IEEE*, and Shiwen Mao, *Senior Member, IEEE*

Abstract—The support for high data rate applications with the cognitive radio technology necessitates wideband spectrum sensing. However, it is costly to apply long-term wideband sensing and is especially difficult in the presence of uncertainty, such as high noise, interference, outliers, and channel fading. In this work, we propose scheduling of sequential compressed spectrum sensing which jointly exploits compressed sensing (CS) and sequential periodic detection techniques to achieve more accurate and timely wideband sensing. Instead of invoking CS to reconstruct the signal in each period, our proposed scheme performs backward grouped-compressed-data sequential probability ratio test (backward GCD-SPRT) using compressed data samples in sequential detection, while CS recovery is only pursued when needed. This method on one hand significantly reduces the CS recovery overhead, and on the other takes advantage of sequential detection to improve the sensing quality. Furthermore, we propose (a) an in-depth sensing scheme to accelerate sensing decision-making when a change in channel status is suspected, (b) a block-sparse CS reconstruction algorithm to exploit the block sparsity properties of wide spectrum, and (c) a set of schemes to fuse results from the recovered spectrum signals to further improve the overall sensing accuracy. Extensive performance evaluation results show that our proposed schemes can significantly outperform peer schemes under sufficiently low SNR settings.

Index Terms—Cognitive radio, sequential detection, wideband sensing, compressed sensing

1 Introduction

Cognitive radio (CR) is attracting growing interest due to its capability of intelligently and dynamically identifying and exploiting spectrum holes to improve the spectral usage efficiency [1], [2]. A core function and essential element of the CR (or secondary user, SU) is to sense spectrum and detect the presence/absence of the primary users (PUs). The growth of high data rate applications such as video makes it attractive to explore holes in a wide spectrum band for transmissions. In addition, some legacy systems constantly change their transmission channels for better performance and security. Thus it is important to enable efficient wideband sensing for CRs to obtain a "wider" spectrum view for more flexible resource access.

A wideband can be generally divided into sub-bands or sub-channels, where the occupancy status by PUs can be determined via sensing of the sub-bands one by one. For a wideband with an extremely large bandwidth (thus a large number of sub-channels), this will bring large overhead and sensing delay. Alternatively, to meet the need of Nyquist sampling rate, CRs can sense the wideband directly with some high-end wideband components, including wideband attenna, wideband radio frequency (RF) front-end and high-speed analog-to-digital converter (ADC). This will inevitably introduce high cost, and may not even be feasible with existing devices. To address this challenge, compressed sensing (CS) [3], [4] is exploited in wideband sensing to reduce the number of samples required [5], [6].

As the activities of PUs are often unknown and dynamic, simple one-time spectrum sensing is inadequate. Under low signal-to-noise ratio (SNR), making a sensing decision simply based on data collected within one time duration either is prone to failure if the sensing duration is not long enough, or suffers from long sensing delay. An SU needs to check the channel status over time, either for in-band sensing where an active SU during its data transmission needs to sense its current channel, or for out-of-band sensing where an SU needs to find an alternate channel. It is important that an SU can make sensing decisions in a timely fashion: for in-band sensing, this helps detect a returning PU rapidly and evacuate the SU from the channel in order not to create significant interference to the PU; for out-of-band sensing, a quick sensing decision saves sensing resources (e.g., sensing time and power) and allows more time for an SU to exploit spectral resources for its data transmissions.

Rather than only considering the sensing algorithm to detect the spectrum activities, it is also very important to determine when and how often to perform sensing. Despite the importance, this is largely ignored in the literature work on wide-band spectrum sensing. Some limited efforts have been made to periodically sense the spectrum of a narrow

- *J. Zhao and X. Wang are with the Department of Electrical and Computer Engineering, Stony Brook University, Stony Brook, NY 11794. E-mail: {jie.zhao, x.wang}@stonybrook.edu.*
- *Q. Liu is with the Computational Sciences and Engineering Division, Oak Ridge National Laboratory, Oak Ridge, TN 37831. E-mail: liuq1@ornl.gov.*
- *S. Mao is with the Department of Electrical and Computer Engineering, Auburn University, Auburn, AL 36849. E-mail: smao@ieee.org.*

Manuscript received 16 Jan. 2017; revised 9 July 2017; accepted 7 Aug. 2017. Date of publication 25 Aug. 2017; date of current version 2 Mar. 2018. (Corresponding author: Jie Zhao.)
For information on obtaining reprints of this article, please send e-mail to: reprints@ieee.org, and reference the Digital Object Identifier below.
Digital Object Identifier no. 10.1109/TMC.2017.2744621

frequency channel [7], [8]; however, it would be very expensive to directly apply CS methods for periodic sensing due to the higher computational complexity for CS recovery. Therefore, despite the advantage in detecting highly agile incumbent signals and facilitating spectrum management, conventional wide-band sensing cannot be directly used to meet the need for long-term sensing, and is costly and inaccurate in the presence of uncertainty, high noise, interference, outliers, and channel fading.

Complementary to existing efforts on wide-band spectrum sensing, in this paper, we focus on the *efficient scheduling* of sensing, in a timely and cost-effective fashion, to detect spectrum usage activities in the presence of uncertain PU activity patterns and varying channel conditions. The major contributions of our work are as follows:

- We propose a novel wideband sensing scheduling scheme, *sequential compressed spectrum sensing*. It incorporates the compressed sensing technique into the sequential periodic sensing framework to take advantage of both for accurate and low-overhead spectrum sensing. Specifically, we perform sequential analysis [9] based on *sub-Nyquist samples* directly without incurring excessive CS recovery overhead, and exploit the sequential detection to improve the sensing performance.
- We investigate a two-stage change-point detection method to quickly and efficiently determine the change in channel usage. In the first stage, sequential sensing is performed to detect the potential change in spectrum occupancy, and in the second stage, intensive in-depth wideband sensing is triggered to make final decisions rapidly on the wideband spectral usage conditions.
- We propose a CS recovery algorithm that exploits the block feature of wideband spectrum to further improve the CS reconstruction performance for more accurate determination of spectrum occupancy conditions.
- We perform extensive simulations to validate and demonstrate the major advantages of our design.

The rest of this paper is organized as follows. After briefly reviewing related work in Section 2, we describe the system model in Section 3. Sequential wideband sensing based on compressed sensing is presented in Section 4 followed by Section 5 where change-point detection and in-depth sensing scheduling are introduced. Section 6 presents our block-sparse recovery algorithm and integrated framework. In Section 7, we present and analyze the simulation results. The paper concludes in Section 8.

2 Related Work

The majority of work on spectrum sensing focus on improving the quality for one-time sensing. From a long-term perspective, the presence of uncertainty, such as high noise, interference, channel fading and anomalies, makes it a daunting task to perform accurate detection solely in one time. Some recent efforts attempt to more accurately sense frequency channels based on a sequence of data with a method such as sequential analysis [9] to detect the spectrum usage conditions at shorter latency and more precise decision. In Kim et al. in [10] and Min et al. in [11], the time is divided into frames each containing a number of sensing blocks, and a decision is made only based on blocks of samples within each frame. Without sensing in the remaining time of the frame after a decision, these schemes are subject to a significant detection delay upon the returning of the legacy users. Guo et al. in [12] proposed a backward sequential probability ratio test which combines the observations from the past several sensing blocks to improve the sensing performance. Rather than fixing the period between sensing blocks without scheduling, a fundamental difference between our work and [10], [11], [12] is that we adaptively schedule sensing over time to speed up the decision while not introducing a high overhead. In [7], [8], the authors show that scheduling periodic sequential sensing helps to improve the spectrum sensing performance. However, it would be very expensive to perform compressed sensing periodically. While there are some studies on change detection [13], [14], they are often decoupled from the sequential spectrum sensing, while there is a need and unique opportunity to put the two together.

Different from existing efforts, one focus of this paper is on effective detection of the activities of legacy wireless systems over a wide spectrum band through smart scheduling of wide-band sensing. The sequential detection is only applied over sparse samples of signals (rather than Nyquist samples) to facilitate low cost coarse signal monitoring, before we determine the actual sub-band occupied by the primary signals. To efficiently detect the change of wide spectrum band, we also adapt the schedule of sequential detection to speed up the detection.

In multiband joint detection [15], primary signals are jointly detected over multiple sub-bands rather than over one large band at a time, where a set of frequency dependent detection thresholds are optimized to achieve the best trade-off between aggregate measures of opportunistic throughput and interference to PUs. As each SU senses the sub-bands one by one, it will incur a long detection delay when the number of sub-bands is large. In addition, the work focuses on the cooperation among SUs in sensing sub-bands. Our work allows an SU to directly sense a wide-band in a long term at low overhead.

Alternatively, compressed sensing is a useful tool for wideband spectrum sensing and analysis. Sub-Nyquist samples are used along with a wavelet-based edge detector in [5] for coarse sensing of wideband to identify spectrum holes, and other wideband spectrum sensing schemes based on CS are proposed in [16], [17], [18]. Sun et al. [6] proposed a multi-slot wideband sensing algorithm with CS and a scheme to reconstruct the wideband spectrum from the compressed samples. Compressive sensing with flexible channel division is proposed in [19], and the authors in [20] make an effort to reduce the computational complexity of compressed sensing with the information from geo-location database. Romero et al. in [21] propose to exploit the second-order statistics such as covariance to improve the compressed sensing performances. Efforts are also made for cooperative wideband sensing [22], [23], [24], [25], [26], [27] with the sensing from multiple users. For example, the algorithm in [24] improves the detection performance and reduces the computational overhead by exploiting the joint sparse properties of wideband signals among multiple SUs.

Although these aforementioned methods show it is promising to apply CS to sensing wide spectrum bands, the complexity involved in CS signal reconstruction makes it difficult for these methods to be used for long-term spectrum monitoring desired by practical cognitive radio systems. Instead, we propose to concurrently exploit sequential detection and compressed sensing for an overall light weight and accurate wideband sensing. Moreover, our framework is not dependent on any particular wideband sampling methodology, and the aforementioned wideband compressed sensing schemes can be applied in our algorithm when there is a need to detect detailed spectrum occupancy conditions in a wideband.

Traditional CS reconstruction algorithms, such as [28] and [29], tend to bring unbearable overhead when the number of samples is utterly large. Taking advantage of the block-sparse feature of signals, in [30], Stojnic et al. proposed a recovery algorithm for block-sparse signals with an optimal number of measurements. Different from existing literature, we design a self-adaptive weighted recovery algorithm based on signal distribution in the spectrum blocks.

The goal of this work is to enable continuous and periodic wideband sensing over time. Rather than simply performing CS recovery during each sensing period, we take advantage of sequential detection and develop various schemes to reduce the recovery overhead and improve sensing performance. Some important issues we consider include: (a) How to better apply CS in sequential wideband sensing to detect spectrum usage conditions without incurring high cost for CS recovery? (b) How to schedule the sequential wideband sensing to reduce the sensing overhead, ensure quick and accurate detection? (c) How to detect the change of spectrum occupancy condition more quickly and accurately? (d) How to more efficiently estimate the wideband spectrum occupancy conditions based on available sensing data?

To answer these questions, we'll first introduce our system model along with some background on wideband spectrum sensing and compressed sensing in the next section.

3 System Model

In a cognitive radio network, secondary users (SUs) can transmit data opportunistically over spectrum unoccupied by primary users. When primary users resume their channel usage, however, CRs are required to evacuate the channel within a predefined time duration. As the activities of PUs could be uncertain and dynamic, a CR needs to sense the channel periodically during its data transmission. In this work, we propose a sequential compressed wideband sensing scheme to enable efficient sensing over a wide spectrum band periodically.

3.1 Wideband Compressed Sensing

A wideband can usually be divided into sub-bands/sub-channels. In the example of Fig. 1, a wide spectrum band ranging from 0 to W(Hz) is equally divided into J sub-bands each with the bandwidth W/J (Hz). In a particular wideband of interest, depending on the activities of different PUs, each sub-band can have different and varying occupancy states. For example, in Fig. 1, sub-bands 2 to 4 are occupied by PU, whereas sub-band J is not. One way to learn the usage conditions of a wide spectrum band is to directly apply the traditional narrow channel detection

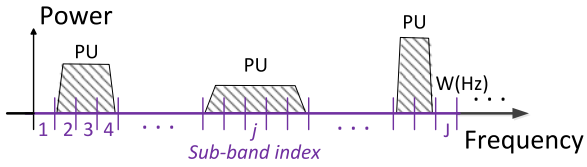

Fig. 1. Frequency division for wideband CRs.

methods to sense the sub-bands one by one. There are many existing studies to decide how to sense the candidate channels. For example, an algorithm proposed by Zhao et al. [31] determines the optimal channel sensing order. For a wideband with a fairly large number of sub-channels, however, sensing channels one by one may bring unacceptable overhead and sensing delay. For example, for a $0 \sim 1$ GHz wideband with each sub-channel occupying 1 kHz, the number of sub-channels is 10^6.

Another way to facilitate wideband spectrum sensing is to equip CRs with essential components such as wideband antenna, wideband RF front-end and high speed ADC to perform sensing over the wideband directly. For wideband sensing, a big challenge is that the required Nyqusit sampling rate can be excessively high. For example, a 0∼500 MHz wideband would result in a Nyquist sampling rate of 1 GHz, which would incur high ADC element costs and processing overhead. This motivates us to exploit CS to significantly reduce the required sampling rate for wideband sensing. In this work, all PUs within the wideband can be regarded as a PU group that occupies part of the sub-channels in the wideband. Throughout this paper, we will use "sub-band" and "sub-channel" interchangeably.

The compressed sensing theory suggests that if an N-dimensional signal is sparse in certain domain, one can fully recover the signal by using only $\Omega(\log N)$ linear measurements. The main idea behind it is to take advantage of the sparsity within the signal to significantly reduce the sampling rate. As a wideband is often sparsely occupied by PUs as shown in Fig. 1, CS can be applied for wideband sensing. For a given wide frequency band of bandwidth W, after obtaining the spectrum occupancy conditions from the sensing, a CR can transmit data exploiting spectral holes.

To detect the spectrum usage condition, a CR can take samples of the received signal $d_{\mathrm{C}}(t)$ for a duration of T_s, where the received signal is composed of PU signals and the background noise. By using a certain sampling rate f_N over the sensing time T_s, we could obtain a discrete-time sequence $d[n] = d_{\mathrm{C}}(\frac{n}{f_N}),\ n = 0, 1, \ldots, N-1$, in a vector form $\mathbf{d} \in \mathbb{C}^{N\times 1}$. Here, $N = T_s f_N$ is usually chosen to be a positive integer. Based on the Nyquist sampling theory, the sampling rate is required to exceed $2W$, i.e., $f_N > 2W$.

To reduce the need of high frequency sampling at the RF front end, in our compressed sensing framework, an SU's detector collects the ambient signal at a certain sub-Nyquist sampling rate f_{sub} smaller than the Nyquist rate f_{nyq}. An $M \times N$ ($M < N$) measurement matrix $\mathbf{\Phi}$ is applied to perform sub-sampling, where M and N denote the number of sub-Nyquist samples and Nyquist samples, respectively. If the sensing period is T_s, then $M = f_{sub}T_s$, $N = f_{nyq}T_s$.

If there is any PU signal within the wideband of interest, the sub-sample vector will be expressed as

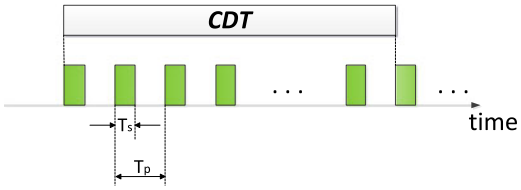

Fig. 2. Channel detection time CDT, sensing period T_p, and sensing time T_s.

$$\begin{aligned}\mathbf{y} &= \mathbf{\Phi}(\mathbf{d}+\mathbf{n}') = \mathbf{\Phi}\mathbf{d}+\mathbf{n} \\ &= \mathbf{\Phi}\mathbf{\Psi}\mathbf{x}+\mathbf{n} = \mathbf{A}\mathbf{x}+\mathbf{n},\end{aligned} \tag{1}$$

where the sub-Nyquist measurements are $\mathbf{y} \in \mathbb{R}^{M\times 1}$, the sparse vector in Fourier spectrum domain $\mathbf{x} \in \mathbb{R}^{N\times 1}$, the additive noise in the wideband $\mathbf{n}'$, the sampled noise $\mathbf{n} \in \mathbb{R}^{M\times 1}$, and the sensing matrix $\mathbf{A} \in \mathbb{R}^{M\times N}$.

Given the measurements $\mathbf{y}$, the unknown sparse vector $\mathbf{x}$ can be reconstructed by solving the following convex optimization problem:

$$\min \quad \|\mathbf{x}\|_{\ell_1} \tag{2a}$$

$$\text{s.t.} \quad \|\mathbf{\Phi}\mathbf{d}-\mathbf{y}\|_{\ell_2} \le \epsilon \tag{2b}$$

$$\mathbf{d} = \mathbf{\Psi}\mathbf{x}, \tag{2c}$$

where the parameter ϵ is the bound of the error caused by noise $\mathbf{n}$, ℓ_p means the ℓ_p-norm ($p = 1, 2, \ldots$). The solution can also be expressed as

$$\hat{\mathbf{x}} = \underset{\mathbf{u}:\ \|\mathbf{y}-\mathbf{A}\mathbf{u}\|_{\ell_2}\le\epsilon}{\arg\min} \|\mathbf{u}\|_{\ell_1}. \tag{3}$$

The signal $\mathbf{d} = \mathbf{\Psi}\mathbf{x}$ can then be recovered as $\hat{\mathbf{d}} = \mathbf{\Psi}\hat{\mathbf{x}}$. In addition to this convex optimization approach (ℓ_1 minimization [28]), there also exist several iterative/greedy algorithms such as Cosamp [29]. Such convex or greedy approaches are generally called the reconstruction algorithms.

It is shown in [32] that if the signal spectrum vector $\mathbf{x} = \mathbf{\Psi}^{-1}\mathbf{d}$ is sparse ($\mathbf{\Psi}^{-1}$ is the Discrete Fourier Transform), then $\mathbf{\Phi} = \mathbf{A}\mathbf{\Psi}$ is essentially an $M \times N$ random sampling matrix constructed by selecting M rows independently and uniformly from an $N \times N$ identity matrix $\mathbf{I}$. This measurement matrix $\mathbf{\Phi}$ can be trivially implemented by pseudo-randomly sub-sampling the original signal $\mathbf{d}$. As we can adopt the inverse DFT matrix as the sparse dictionary $\mathbf{\Psi}$, the measurement matrix will be reflected by sub-Nyquist sampling. For a time domain signal with the length N, this sub-Nyquist measurement corresponds to a smaller sampling number $M < N$. If the spectral sparsity level K of $\mathbf{x}$ is known, one can choose the number of measurements M to secure the quality of spectral recovery.

3.2 Periodic Sensing over Time

To support practical transmissions, the spectrum needs to be continuously monitored. The spectrum sensing can be carried out periodically as in Fig. 2, and the intervals between sensing may also vary to speed up the detection as we will show later. To not interfere with the legacy occupants, secondary users need to timely evacuate the channel. Thus the channel detection time (CDT) is defined as the maximum allowed time for a sensing decision to be made.

We consider periodic *in-band channel sensing*, with the sensing performed by an SU periodically during its transmissions. In each period T_p, an SU will use part of the time T_s for sensing, and the remaining time for transmissions. A CDT usually includes multiple sensing-transmission periods T_p. To enure a sensing decision to be made within a CDT, we have $T_p \le CDT$ so that the channel is sensed at least once during a CDT period. Our major focus is to develop an efficient wideband sensing scheme to enable long-term channel monitoring at low cost. Our scheme will facilitate SUs to continuously transmit data packets over opportunistic spectrum, but the scheduling of transmissions of SUs is beyond the scope of our work.

The *sensing overhead* (R_{so}) describes the proportion of time dedicated to the sensing task and is defined as the ratio between T_s and T_p, i.e., $R_{so} = T_s/T_p$. Sensing scheduling will have a significant impact on sensing overhead. Instead of making a sensing decision independently within each T_p, to improve the sensing quality, we will take the sequential detection using consecutive groups of samples.

In order to make more precise decision under low signal to noise ratio through sequential wideband sensing, a straightforward method is to directly combine the compressed sensing and the periodic sensing together. With this method, Nyquist samples of PU signals can be recovered through $\hat{\mathbf{d}} = \mathbf{\Psi}\hat{\mathbf{x}}$ in each period with $\hat{\mathbf{x}}$ first obtained from CS reconstruction using the sub-Nyquist samples, then Nyquist samples are further processed through a sequential detection algorithm to determine the channel occupancy condition. Once detecting the existence of legacy users, the occupation status of each sub-band is determined based on the sensed power of certain sub-bands of the recovered $\mathbf{x}$.

Recovering samples through CS in each small sensing period T_p, however, would introduce a high computational overhead. Instead, we propose a Sequential Wideband Compressed Sensing (SWCS) algorithm which directly applies compressed samples to make the sequential detection first, and only after the wideband channel is determined to be occupied by PUs will CS recovery be pursued. We will introduce the details of our algorithm in the next section.

4 Sequential Wideband Compressed Sensing

In this section, we introduce the basic techniques we use for sequential detection with compressed samples.

4.1 Sequential Detection with a Group of Sub-Sampled Data

Unlike the traditional one-time detection, in a sequential detection, a detector sequentially observes data over time and decides, at each step, whether it has collected sufficient observations to make a reliable detection decision (e.g., if PUs are present in the band sensed) that it can stop making more observations; otherwise, the detector continues to the next step with more observations till either a decision is made or the detector has collected the maximum amount of data allowed. In this work, our major task is to detect if there exist PU signals in the wide spectrum band and then analyze the usage conditions of the wideband spectrum.

As a classic sequential detection method, Wald's Sequential Probability Ratio Test (SPRT) [9] aggregates the log-likelihood ratio of the i.i.d. samples till either of two predefined constant thresholds is reached. For the given false alarm and missed detection probabilities P_{FA} and P_{MD}, among

all the tests, Wald's SPRT is proven to require the fewest samples in one test run on average. In this work, we propose the use of *grouped-compressed-data SPRT* (GCD-SPRT), with data samples within each T_s being grouped together to form a "super-sample" to reduce the effect of short-term channel randomness as a result of multi-path fading.

Our proposed scheme takes advantage of compressed sensing to reduce the sampling cost. A major difference between our work and related work lies in two aspects: 1) compared to the conventional sequential detection, we use compressed samples instead of raw samples from Nyquist sampling in the detection process, which avoids using the high end A/D in wideband sensing; and 2) rather than straight-forwardly recovering data through CS for each sampling group and using the recovered Nyquist-rate samples in the sequential detection, our scheme only performs spectrum recovery when the spectrum analysis is needed after having determined the spectrum is occupied or likely to be occupied, which avoids the high recovery overhead. In this section we first introduce the basic procedures of our GCD-SPRT and then analyze its features.

4.1.1 Procedures of GCD-SPRT

The basic steps in GCD-SPRT can be summarized as follows:

Step 1: Find the power $y(\mathbf{x})$ from M sub-Nyquist samples.

If there is any PU signal within the wideband of our interest, the sub-sample vector will be expressed as in Eq. (1). The normalized power of M sub-Nyquist samples contained within a sensing block T_s is

$$z(\mathbf{y}) = \frac{\sum_{i=1}^{M} y_i^2}{T_s}, \tag{4}$$

where y_i denotes the individual samples within T_s. Recall that $M = f_{sub}T_s$, then Eq. (4) can be rewritten as

$$z(\mathbf{y}) = \frac{f_{sub}}{M}\sum_{i=1}^{M} y_i^2. \tag{5}$$

In practice, the number of samples taken within a single T_s is fairly large. For example, for $T_s = 1$ ms and a 0∼500 MHz wideband, the Nyquist sample number will be $N = 10^6$; and even if we perform sub-sampling with 1/10 of the Nyquist sampling rate, we will have 10^5 sub-Nyquist samples. With the Law of Large Numbers ($M \gg 10$), we have

$$z(\mathbf{y}) \overset{i.i.d.}{\sim} \begin{cases} H_0 : \mathcal{N}\Big(f_{sub}P_n, \frac{(f_{sub}P_n)^2}{M}\Big), \\ H_1 : \mathcal{N}\Big(f_{sub}P_n(1+SNR), \frac{(f_{sub}P_n)^2(1+SNR)^2)}{M}\Big). \end{cases} \tag{6}$$

Here, SNR is defined as the ratio between the nominal signal power P and local noise floor $\sigma^2 = P_nW$, where P_n is the noise power spectral density (PSD) and W is the bandwidth. The power samples taken with the duration T_s is approximately Gaussian regardless of the original distribution of the PU signal.

If Nyquist-equivalent samples are recovered from the sub-samples by CS, then similar to Eq. (4), the power of N recovered Nyquist-equivalent samples within T_s is

$$z_{nyq}(\mathbf{y}) = \frac{\sum_{i=1}^{N} y_i^2}{T_s}, \tag{7}$$

where y_i denotes the Nyquist-equivalent samples within T_s. The distribution of $z_{nyq}(\mathbf{y})$ is a little different from that in Eq. (6). Specifically, f_{sub} is substituted by Nyquist rate f_{nyq}, M is substituted by Nyquist sample number N, and the mean of the Gaussian distribution will also be different due to the fact that the recovered samples are essentially the estimated PU signal samples:

$$z_{nyq}(\mathbf{y}) \overset{i.i.d.}{\sim} \begin{cases} H_0 : \mathcal{N}\Big(0, \frac{(f_{nyq}P_n)^2}{N}\Big), \\ H_1 : \mathcal{N}\Big(f_{nyq}P_nSNR, \frac{(f_{nyq}P_n)^2(1+SNR)^2)}{N}\Big), \end{cases} \tag{8}$$

We'll introduce later in our scheduling design when to use compressed samples and when to use recovered samples to perform GCD-SPRT.

Step 2: Derive the test statistic for each group of samples.

The test static $T(z(\mathbf{y}))$ is defined as the log-likelihood ratio (LLR) of the power sample and represented as

$$T(z(\mathbf{y})) = \ln\frac{f_1(z(\mathbf{y}))}{f_0(z(\mathbf{y}))}, \tag{9}$$

where $f_0(\cdot)$ and $f_1(\cdot)$ are the probability density functions (PDFs) under H_0 and H_1, respectively, as indicated in Eq. (6). As we will deal with the power sample $z(\mathbf{y})$ directly, for ease of presentation, we will simply refer $z(\mathbf{y})$ as z.

Step 3: Spectrum occupancy decision with the aggregate test statistic $\mathcal{T}$.

Each T from Step 2 corresponds to one group of data. For the sth group, we have

$$T(z_s) = \ln\frac{f_1(z_s)}{f_0(z_s)}. \tag{10}$$

By accumulating $T(z_s)$ $(s = 1, 2, \ldots)$ sequentially, the aggregate test statistic up to the sth group is

$$\mathcal{T}_s = \sum_{k=1}^{s} T(z_k) = \sum_{k=1}^{s} \ln\frac{f_1(z_k)}{f_0(z_k)}. \tag{11}$$

To determine the spectrum occupancy status, we choose the two decision thresholds as those in Wald's SPRT:

$$A = \ln\frac{P_{MD}}{1-P_{FA}}, \text{ and } B = \ln\frac{1-P_{MD}}{P_{FA}}. \tag{12}$$

The decision rule for the SU is

- if $\mathcal{T}_s > B$, it decides that the PU has reclaimed the channel.
- if $\mathcal{T}_s < A$, it decides that the channel is still available;
- otherwise, it goes to *Step 1* to continue to sample another group of power data, and update $\mathcal{T}_{s+1}$ using Eq. (11).

The *stopping time/run length* S is defined as the minimum number of steps after which one of the two decision thresholds is first crossed; that is,

$$S = \min\{s : \text{ either } \mathcal{T}_s < A \text{ or } \mathcal{T}_s > B\}. \tag{13}$$

A smaller S means that the SU can make its detection decisions faster, which in turn guarantees that the SU can (1) spend less time performing detection, (2) evacuate the channel in a timely fashion so as not to severely interfere with the reappearing PUs, and (3) dedicate more time to data transmission for enhanced throughput.

4.1.2 Analysis on Run Length and Overhead

In this section, we provide a list of analytical results for the sequential detector as described in the last section, including the expected values of the test statistics, the average run steps and the average sensing overhead. The proofs in this section are omitted due to space constraint.

Proposition 1. *Each of the i.i.d. test statistics $T(z)$ has the expected values*

$$m_0 \triangleq \mathbb{E}[T(z)|H_0] = -\frac{M-1}{2}\frac{SNR^2}{(1+SNR)^2} + \frac{SNR}{(1+SNR)^2} - \ln(1+SNR), \tag{14}$$

and

$$m_1 \triangleq \mathbb{E}[T(z)|H_1] = \frac{M+1}{2}SNR^2 + SNR - \ln(1+SNR), \tag{15}$$

under H_0 and H_1, respectively.

The above m_0 and m_1 are the average increments at each step of the sequential test. For a given M, both values depend solely on SNR. The average speed of the sequential test has a direct bearing on the separation of the two underlying distributions. In fact, thanks to the independence of different sample groups, we have

$$-I_{01} = \mathbb{E}\left[\ln\frac{f_1(T)}{f_0(T)}|H_0\right] = \int f_0(u)\ln\frac{f_1(u)}{f_0(u)}\,\mathrm{d}u. \tag{16}$$

Intuitively, as the SNR increases, the two hypotheses can be separated from each other faster.

By plotting both m_0 and m_1 under variable SNR values, we observe that $|m_0| < |m_1|$ and both $|m_0|$ and $|m_1|$ increase monotonically with SNR. With low channel SNRs, that is, $SNR \to 0^+$, we have $1 + SNR \approx 1$ and $\ln(1+SNR) \approx SNR$. Plugging these two equations into Eqs. (27) and (15), we have

$$m_0 \approx -\frac{M}{2}SNR^2, \text{ and } m_1 \approx \frac{M}{2}SNR^2. \tag{17}$$

That is, the absolute values of the average increments under H_0 and H_1 are roughly the same when the channel SNR is low; in other words, the underlying sequential test runs at the same rate under both hypotheses.

In general, the exact distribution of the test statistic is difficult to derive; however, when the SNR is low, the distributions under H_0 and H_1 can be approximated as Gaussian, as shown below.

Proposition 2. *Under low-SNR conditions, we have*

$$T(z) \overset{i.i.d.}{\sim} \begin{cases} H_0 : \mathcal{N}(m_0, 2m_1), \\ H_1 : \mathcal{N}(m_1, 2m_1), \end{cases} \tag{18}$$

in which m_0 and m_1 are given in Eq. (17).

From Eq. (18), the test statistics under H_0 and H_1 are symmetric around zero: they have equal variances and opposite means. This means it would take, on average, the same number of steps for a sequential test to hit either the lower or upper decision boundary.

Next we consider the average run length—the average number of sample groups that need to be collected in order to reach either decision threshold.

Proposition 3. *Regardless of the SNR value, the average run lengths S for the SU to make a decision on the channel state under H_0 and H_1 are*

$$\mathbb{E}[S|H_0] = \frac{P_{FA}B + (1-P_{FA})A}{m_0} \tag{19}$$

$$\text{and } \mathbb{E}[S|H_1] = \frac{(1-P_{MD})B + P_{MD}A}{m_1}, \tag{20}$$

respectively.

From Eqs. (12), (19), and (20), when $P_{FA} = P_{MD}$, we have $A + B = 0$ and $\mathbb{E}[S|H_0] = \mathbb{E}[S|H_1]$. That is, the sequential test has a symmetric structure and it takes an equal number of steps on average to reach either decision boundary. If more strict requirement is imposed on P_{MD} to ensure the interference minimal to the PUs, that is, $P_{MD} \ll P_{FA}$, we would have $|A| >> |B| \approx -\ln P_{FA}$. In this case, even with nearly identical increments $|m_0| = |m_1|$ when the channel SNR is very low, the upper threshold takes much less time to be crossed. Thus, when the PU is indeed present, the SU is expected to quickly make the correct decision.

From Eqs. (17), (19), and (20), the expected numbers of samples for running one sequential test under H_0 and H_1 with low channel SNRs are

$$M * \mathbb{E}[S|H_0] \approx -\frac{2((1-P_{FA})A + P_{FA}B)}{SNR^2} \tag{21}$$

$$\text{and } M * \mathbb{E}[S|H_1] \approx \frac{2((1-P_{MD})B + P_{MD}A)}{SNR^2}, \tag{22}$$

respectively. If both Eqs. (21) and (22) are multiplied by the sampling period—the inverse of the sampling frequency—we have the total expected time spent on sensing. For a given time frame to complete the detection task, say CDT, the expected sensing overhead ρ under both hypotheses can also be obtained

$$\mathbb{E}[\rho|H_0] = T_s/CDT * \mathbb{E}[S|H_0], \tag{23}$$

$$\mathbb{E}[\rho|H_1] = T_s/CDT * \mathbb{E}[S|H_1]. \tag{24}$$

To summarize the results in this section, for a single run of the GD-SPRT, we have the following relationships: For a given channel SNR value, the number of samples M and the expected run length $\mathbb{E}[S]$ are inversely proportional under either hypothesis; as such, the expected sensing overhead $\mathbb{E}[\rho|H_0]$ and $\mathbb{E}[\rho|H_1]$ are fixed. The overhead under each hypothesis is in turn proportional to SNR^{-2}. If the channel SNR is reduced by 5 dB, for instance, the average number of samples required to maintain the same sensing accuracy level would be 10 times the original.

4.2 Backward GCD-SPRT with Scheduling

So far we have only introduced our group-based sequential test without considering how the groups of data can be scheduled for sampling over time. If the GCD-SPRT is applied over time for periodic sensing, the sensing process may have a structure shown in Fig. 3a. Time is divided into non-

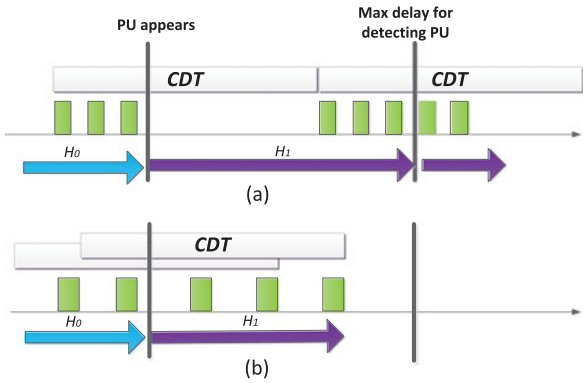

Fig. 3. Detection delay (purple arrows) with sensing scheduling (a) forward, non-overlapping GCD-SPRT and (b) backward, overlapping GCD-SPRT.

overlapping units, each with length CDT. The GCD-SPRT runs within each window till either threshold is crossed. As long as an H_0 decision is made, the rest of the CDT period can be dedicated to uninterrupted secondary data transmission.

As no samples are taken after a decision is made within a period, if some PUs resume the usage of their channels in the remaining part of the period, they will not be detected until enough samples are taken in the new period. This not only introduces a delay in the decision making, but the overall duration from the reappearance of a PU until the decision making may exceed the CDT limit.

In contrast to the scheme in Fig. 3a, in our design, after collecting new sensing data after every T_p, the SU updates its sensing decision. That is, we let the CDT-window slide forward by T_p after a new group of data has been collected, as shown in Fig. 3b. As the CDT-window moves forward, a GCD-SPRT can run *backward* at each position of the CDT-window, starting from the latest group of data. Since the newest data within the current window might be generated under a different distribution from the older ones, by having each sequential test run backward, we reduce the impact of the older sensing data in the CDT-window that might obscure the effect of the newer ones so that a possible status change can be detected faster.

Both the forward and backward running schemes described above are illustrated in Fig. 3. Here, the PU reappears right after the sensing action ended in one of the non-overlapping CDT periods. In (a), as the channel goes undetected until the next window, the evacuation delay of the SU may exceed the required length CDT, thereby violating the system requirement. On the other hand, in (b), the returning PU might be detected earlier before the evacuation deadline, thanks to the closer intervals between adjacent sensing groups. In both schemes, the interval T_p can be determined based on N, which is in turn estimated based on the given thresholds of false alarm (P_{FA}) and missed detection (P_{MD}) probabilities. The schedule is not changed during the sensing process. In our work, we propose further actions taken by the SU, where the sensing frequency (determined by T_p) is increased after a possible PU return is suspected, which results in even faster channel evacuation for in-band sensing. We defer the detailed design of this change detection to Section 5.

5 Quick Change Detection

It is important to quickly detect the "change point" where the wideband state shifts from H_0 to H_1 due to PU reappearance. Generally, CRs are required to evaluate channel within a given time duration. In order to speed up the change point detection, we propose an in-depth sensing method in which a CR adjusts its sensing frequency and method to ensure more rapid and precise detection after suspecting the possible H_0-to-H_1 transition.

5.1 Detection of Possible Change

From Eq. (6), the mean value under H_1 is $(1 + SNR)$ times that under H_0, where SNR is defined as the ratio between the nominal signal power P and local noise floor $\sigma^2 = P_n W$. In a low-SNR case, the mean under both H_1 and H_0 would be very close within a sensing block time T_s.

By collecting data from different sensing blocks and comparing them, the SU may be able to gather information that first indicates (1) a sufficient number of test statistic values have been collected that the total shifts towards either of the detection thresholds, and (2) this shift is consistent, whereupon a change in channel status is suspected. We set the following criteria to determine when the *in-depth sensing* should be triggered to speed up the change detection

$$\begin{aligned}\mathcal{T}_c &= \max\{\bar{T}_{new} - \bar{T}_{old}\} \geq \delta\left(n_{new}\frac{B}{n} - n_{old}\frac{A}{n}\right) \\ &= \delta(n_{new}B - n_{old}A)/n,\end{aligned} \tag{25}$$

where $\mathcal{T}_c$ is the test statistic that will trigger the in-depth sensing; $\bar{T}_{new}$ and $\bar{T}_{old}$ are the summation of the newer and older test statistics in the CDT-window respectively, and n_{new} and n_{old} ($n = n_{new} + n_{old}$) are the numbers of test statistics classified as newer and older in the CDT-window respectively; B and A are the thresholds in Eq. (12), and δ is the parameter that controls the sensitivity of an SU to the shift. With a smaller δ, the SU is more sensitive to the changes in the observed data.

Now we explain how to classify test statistics as "new" and "old". A test statistic is obtained within a T_s. For a given set of test statistics in the CDT-window, the SU starts with the most recent one as "new" while setting the remaining sensing blocks in the window as "old" and calculates their difference; then the new test statistic set includes the second most recent test statistic, with the "old" minus this test statistic, so the numbers of newer test statistics and older ones are increased and decreased by one respectively. This test continues until the data from a CDT-window have all been checked. If Eq. (25) is still not met, then regular GCD-SPRT-based sequential detection is pursued; otherwise, the in-depth sensing is performed.

Despite their different goals, the regular and change detection processes are integrated into a single framework in our Compressed-Sensing-based sequential periodic sensing design. During regular sensing, as a new group of energy samples is taken, the test statistic is calculated.

5.2 In-Depth Sensing

An SU will take the in-depth sensing after an H_0/H_1 state change is suspected. There are many ways to schedule the in-depth sensing, as long as the sensing process can be carried out more accurately and robustly than the regular periodic sensing process. In our design, we not only adapt the sensing frequency by adjusting T_p but also use the recovered samples instead of compressed samples to facilitate more accurate sequential detection.

The backward running GCD-SPRT with the schedule change is illustrated in Fig. 5, where we can observe the increase of sensing frequency when a change is suspected after sufficient data have been accumulated. An SU can adjust its sensing period from T_p to $T_{p,1}$ and then from $T_{p,1}$ to $T_{p,2}$ ($T_p > T_{p,1} > T_{p,2}$), in order to expedite the final detection decision. Sensing scheduling enables the SU to gather more samples when possible PU appearances are suspected and thus determine the occupancy of the spectrum in a timely manner. Next we discuss some issues to be considered.

5.2.1 What Value Should the New T_p be Adjusted to

As discussed earlier, due to many higher-layer concerns such as coordination and synchronization, generally T_p is set to a discrete value in a practical system.

The sensing period T_p can be set according to the number of steps needed to reach one of the thresholds

$$T_p = \frac{CDT}{A} m_0, \tag{26}$$

where m_0 is defined as the average increment of test statistic $T(z)$ at each step of the sequential test under H_0

$$\begin{aligned} m_0 &\triangleq \mathbb{E}[T(z)|H_0] \\ &= -\frac{M-1}{2}\frac{SNR^2}{(1+SNR)^2} + \frac{SNR}{(1+SNR)^2} - \ln(1+SNR). \end{aligned} \tag{27}$$

Similar to the T_p setting in 802.22 WRAN, in our sensing scheduling, we choose an appropriate discrete T_p that is the integer multiples of a MAC frame size FS. In general T_p cannot be too large or too small. If it is too large, higher sensing delay will be introduced; if too small, the temporal diversity in periodic sensing model is not effectively exploited and the sensing overhead will also be high.

To speed up the sensing process during in-depth sensing, we set the multiple to be a predefined small value. We will study the impact of the T_p adjustment on performance in simulations.

5.2.2 When to Recover Samples in Order to Make Decision of Sequential Detection

There are two major benefits associated with the recovery of the Nyquist-equivalent samples from compressed samples: (1) we can have more reliable test statistics to conduct SPRT, and (2) if a wideband is determined to have PU occupancy, CS recovery can help analyze the spectrum usage and determine which sub-bands are occupied by recovering the spectral domain signal. Trade-offs exist in selecting an appropriate CS recovery time: on the one hand, if an SU recovers samples too soon, it may experience a higher recovery overhead; on the other, if CS recovery is pursued too late, it may result in too long a sensing delay.

We consider the scheme of *shift-window-based recovery* that is taken after suspecting a channel status change. Samples are not recovered and used to make decisions until the CDT-window slides forward by the original T_p. If the new T_p is smaller than the old one, it is likely that more than one group of data need to be recovered to serve as test statistics. The newly recovered test statistics are aggregated with the other groups of recovered test statistics in the CDT-window to perform the sequential detection. This method essentially allows SU to collect more groups of recent data for a decision.

We will discuss how to effectively recover the wideband spectrum from sensed samples in the next section.

Algorithm 1. SWCS

1: Initialization: the pseudo-random sub-Nyquist measurement matrix $\mathbf{\Phi}$ as described in Section 3.1
2: For each sensing block T_s, sub-sample with $\mathbf{\Phi}$, collect sub-Nyquist samples $\mathbf{y}$ expressed in Eq. (1).
3: Calculate test statistics described in GCD-SPRT and perform change detection.
4: **if** Eq. (25) is not met **then**
5: Perform regular Backward GCD-SPRT with fixed T_p described in Section 4 until the decision on PU status can be made.
6: **else**
7: Change is suspected and in-depth sensing is triggered. Adapt sensing period T_p.
8: Perform CS recovery with a traditional CS algorithm, e.g., ℓ_1 minimization in [28] and Cosamp in [29].
9: Use the recovered Nyquist-equivalent samples in Backward GCD-SPRT for the sequential sensing until the decision on PU status can be made.
10: **end if**
11: **if** PU is detected to be present **then**
12: **if** If in-depth sensing has not been triggered thus there is no CS recovery **then**
13: Reconstruct the most recent group of samples to analyze the spectral usage of each sub-band in the wideband.
14: **else**
15: The sub-bands recovered in multiple periods during in-depth sensing are fused to analyze the spectral usage of each sub-band in the wideband (Section 6.2).
16: **end if**
17: **end if**

6 Recovery of Block-Sparse Wideband Spectrum

CS recovery from the sparse samples is needed in in-depth sensing phase to make quick detection of spectrum occupation change, and also needed to determine the detailed spectrum occupancy conditions inside the wideband. Instead of simply using traditional CS recovery algorithms such as [28] and [29], we design our recovery algorithm based on the wideband signal's feature, i.e., block sparse properties of the wideband spectrum.

In our framework, the measured signal in the frequency domain exhibits the characteristics of block sparsity, as shown in Figs. 1 and 4, which motivates us to use the block sparse properties to help reconstruct the signal.

6.1 Weighted Block Recovery

To exploit the block structure, instead of solving a ℓ_1 optimization problem in (2), the following problem can be solved:

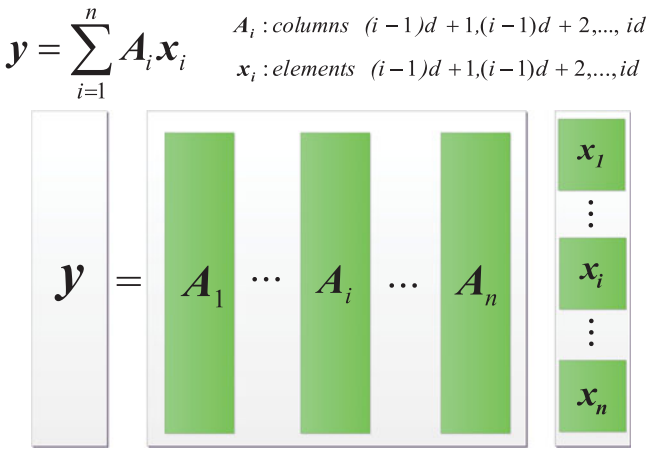

Fig. 4. Block sparse model.

$$\begin{aligned} \min \quad & \sum_{i=1}^{n} \|\mathbf{X}_i\|_2 \\ \text{subject to} \quad & \mathbf{Ax} = \mathbf{y}, \end{aligned} \tag{28}$$

where $\mathbf{X}_i = x_{(i-1)d+1:id}$. Fig. 4 illustrates the main idea of block partition. A vector $\mathbf{x}$ represents the sparse power spectrum of the wideband with nd elements. It is partitioned into n blocks, each consisting of d elements. $\mathbf{X}_i$ is the ith spectrum block. $\mathbf{A}$ is the sensing matrix, and its ith partition $\mathbf{A}_i$ corresponds to the ith spectrum block $\mathbf{X}_i$.

To further improve the reconstruction performance, instead of equally treating all the channel blocks, we give a block with potentially higher energy a lower weight so its recovered gain value is less restricted. We solve the following problem in our design:

$$\begin{aligned} \min \quad & \sum_{i=1}^{n} w_i \|\mathbf{X}_i\|_2 \\ \text{subject to} \quad & \mathbf{Ax} = \mathbf{y}, \end{aligned} \tag{30}$$

where w_i is a weighted factor for block $\mathbf{X}_i$.

We propose a weighted-block-sparse recovery algorithm in Algorithm 2 to assign weights to each block and update the weights through iteratively solving (30). Weights are increased for the blocks not likely to contain many non-zero elements, so that when solving the minimization problem in (30) those likely-zero blocks can be dragged down; for the blocks that are likely to be non-zero, weights are reduced to relax those blocks. Our algorithm improves the wideband sensing performance from two aspects: (a) noise reduction by disregarding data from likely-zero blocks (frequency bands) as in Algorithm 2; (b) weight update through each iteration to improve the accuracy.

6.2 Determination of Wideband Power Spectrum Usage

After detecting that PUs are present in the wideband through sequential detection, we need to determine which subbands are occupied. If the PUs are detected without in-depth sensing in Section 5.2 (e.g., the PUs are likely to be either absent from the wideband or have already been present in the wideband before detection starts), we can apply the group of compressed samples in the most recent sensing period T_p to reconstruct the wideband power spectrum

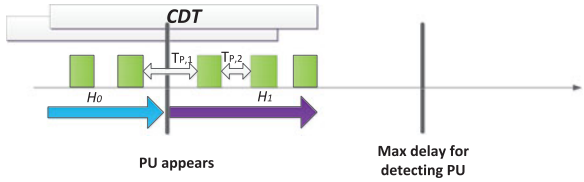

Fig. 5. Detection delay (purple arrows) with sensing scheduling: backward, overlapping GCD-SPRT with short-term T_p adjustment.

usage. If in-depth sensing is triggered and compressed samples in different sensing period T_p are reconstructed to facilitate the sequential detection, it remains an issue how to fuse the recovery results from T_p to determine the wideband power spectrum usage.

Algorithm 2. Reconstruction of Block Sparse Signals

1: Initialization: measured vector $\mathbf{y}$, size of blocks d, and measurement matrix $\mathbf{A}$.
2: **if** Termination condition is not met **then**
3: Solve the following optimization problem using semi-definite programming

$$\begin{aligned} \min_{\mathbf{x}} \quad & \sum_{i=1}^{n} w_i \|\mathbf{X}_i\|_2 \\ \text{subject to} \quad & \mathbf{Ax} = \mathbf{y}, \mathbf{x} = [\mathbf{X}_1, \mathbf{X}_2, \ldots, \mathbf{X}_n]. \end{aligned} \tag{29}$$

4: Sort $\mathbf{X}_i$ such that $\|\mathbf{X}_{j_1}\|_2 \geq \|\mathbf{X}_{j_2}\|_2 \geq \cdots \|\mathbf{X}_{j_n}\|_2$.
5: Update $\hat{\mathbf{A}}$ to be the submatrix of $\mathbf{A}$ containing columns of first $(K-1)d$ rows of $\mathbf{A}$ that corresponds to the blocks $j_1, \ldots, j_{K-1}$.
6: Update $\mathbf{y} \leftarrow \hat{\mathbf{A}}\mathbf{x}$ (Disregard the weakest block information from measurements.)
7: Calculate $\mathbf{x} = \hat{\mathbf{A}}^{-1}\mathbf{y} = [\mathbf{X}_1, \mathbf{X}_2, \ldots, \mathbf{X}_n]$.
8: For each block $\mathbf{X}_i$, count the number of $\mathbf{x}$ entries that are above a predetermined threshold m_i.
9: Update the weight of each block w_i: $w_i \leftarrow \frac{\sum_{i=1}^{n} m_i}{m_i}$.
10: **end if**
11: Output the recovered signal $\mathbf{x} = [\mathbf{X}_1, \mathbf{X}_2, \ldots, \mathbf{X}_n]$.

In CS recovery, we first recover the spectrum domain signals, which can form the map to indicate which subbands are occupied. The Nyquist-equivalent samples can be obtained through the inverse DFT. A recovery example under $SNR = -5$ dB is shown in Fig. 6. An SU analyzes the occupancy states of the sub-bands based on the recovered spectral energy level.

After a change is suspected, a set of spectral domain signals will be recovered before the final sensing decision is made, each spectrum signal is reconstructed from the compressed data of one T_p. Thus, there will be a set of spectral maps accordingly. In addition, when SNR is relatively low (e.g., -5 dB as in Fig. 6), the recovered spectrum contains some incorrect spikes due to noise. Traditional CS-based wideband analysis usually assumes relatively high SNR (e.g., 20 dB), which may not be practical. In the case of relatively low SNR, to alleviate the effects of noise and make the sub-band analysis more accurate, multiple recoveries from different sensing periods can be applied to perform the sequential detection on spectrum occupancy conditions. There needs a way to fuse these recovered spectrum maps. We consider two candidate fusion schemes:

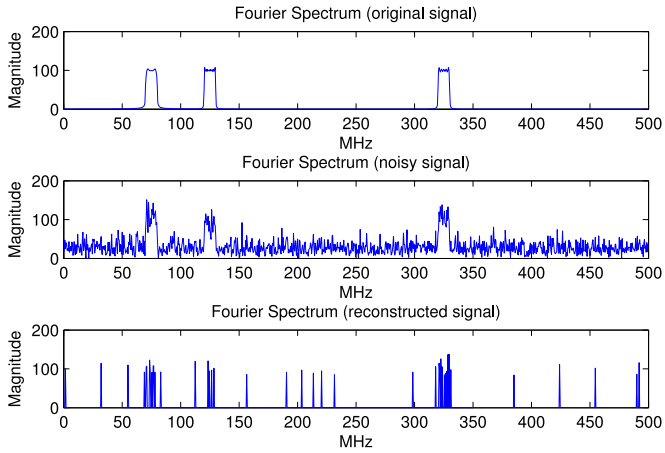

Fig. 6. CS recovery in a T_s under $SNR = -5$ dB.

(a) *Data Fusion*. Regardless of the algorithm assumed for initiating CS sample recovery, an SU calculates the average energy of the set of recovered power spectrum data. The average energy value of each sub-band is compared with an energy threshold. A binary map is applied to represent if a sub-band is occupied, one if a sub-band has its energy above the threshold, 0 otherwise.

(b) *Decision Fusion*. The spectrum energy map from each recovery is applied to determine which sub-bands are occupied first. Then the SU merges the maps by OR rule, AND rule, or majority rule, among others.

In this paper we consider signal recovery. For sub-band status analysis purposes, support recovery may be enough if the goal is only to identify whether the sub-band is occupied rather than the specific power level in that sub-band. Many references (e.g., [33] demonstrate that the support recovery is generally more robust to noise and errors than the signal recovery. Support recovery methods can be trivially implemented on top of our design.

6.3 An Integrated Framework

We have introduced different design components, and we will now present the integrated framework. To perform an efficient sequential detection, our algorithm from Section 4 monitors all the data within the current CDT-window and performs the change detection in Section 5 to determine whether the in-depth sensing in Section 5.2 should be triggered. If not, the regular sensing is performed; otherwise, the in-depth sensing is run until either an H_0 or H_1 decision is made and the sensing period is reset to the original level. If H_1 decision is made, the power spectrum of the wideband will be analyzed to determine the state of each sub-band. The power spectrum analysis is done through the recovery of the sparse spectrum signal from the sub-sampled data, for which we apply a weighted block-sparse recovery algorithm in Section 6 instead of using the traditional compressed sensing reconstruction solution. Based on different CS reconstruction algorithms, we propose two frameworks summarized in Algorithm 1 and Algorithm 3. Although both have our sequential detection structure, the difference between the two is that Algorithm 1 (SWCS: Sequential Wideband Compressed Sensing) exploits the traditional CS recovery algorithm without considering the block sparsity, whereas Algorithm 3 (SWCS-BS: Sequential Wideband Compressed Sensing with Block Sparsity) uses our proposed weighted block-sparse CS recovery algorithm in Algorithm 2. We will compare the performances of SWCS and SWCS-BS in simulations.

Algorithm 3. SWCS-BS

1: Initialization: the pseudo-random sub-Nyquist measurement matrix $\mathbf{\Phi}$ as described in Section 3.1
2: For each sensing block T_s, sub-sample with $\mathbf{\Phi}$, collect sub-Nyquist samples $\mathbf{y}$ expressed in Eq. (1).
3: Calculate test statistics described in GCD-SPRT and perform change detection.
4: **if** Eq. (25) is not met **then**
5: Perform regular Backward GCD-SPRT with fixed T_p described in Section 4 until the decision on PU status can be made.
6: **else**
7: Change is suspected and in-depth sensing is triggered. Adapt sensing period T_p.
8: Perform CS recovery with the proposed block sparse reconstruction algorithm in Algorithm 2.
9: Use the recovered Nyquist-equivalent samples in Backward GCD-SPRT for the sequential sensing until the decision on PU status can be made.
10: **end if**
11: **if** PU is detected to be present **then**
12: **if** If in-depth sensing has not been triggered thus there is no CS recovery **then**
13: Reconstruct the most recent group of samples to analyze the spectral usage of each sub-band in the wideband.
14: **else**
15: The sub-bands recovered in multiple periods during in-depth sensing are fused to analyze the spectral usage of each sub-band in the wideband (Section 6.2).
16: **end if**
17: **end if**

7 Simulations and Results

In this section, we conduct MATLAB simulation studies to demonstrate the performance of our design. We first investigate the performances of SWCS to evaluate the effectiveness of our in-depth sensing scheduling, and then assess SWCS-BS to see the advantages of exploiting block-sparse properties of wideband.

We will compare our scheduled sequential wideband sensing design with non-scheduled method and also look into some peer schemes to investigate the advantages of SWCS scheduling. As our framework focuses on scheduling of sequential sensing, its compressed sensing component does not rely on any specific CS-based spectrum detection scheme. We do not compare SWCS with various existing wideband sensing schemes on CS sampling and recovery design, but rather focus on evaluating the benefits as a result of sensing scheduling using a basic CS algorithm.

7.1 Simulation Settings

7.1.1 System Setup

We consider a wideband of 500 MHz, which can be virtually divided into 50 sub-bands, each occupying 10 MHz. The

TABLE 1
Default Sensing Scheduling

PU energy level (dB)	−23.8	−22.8	−21.8	−20.8	−19.8	−18.8
Tp/FS	5	7	12	19	29	46

Nyquist sampling rate is 1 GHz. A PU group signal is a wideband signal that spreads over the wideband, but may only occupy a small portion of the wideband, i.e., the number of occupied sub-bands is much smaller than the total number of sub-bands monitored. The noise is assumed to be circular complex AWGN, i.e., $\mathbf{n} \sim \mathcal{N}(0, \eta^2)$. SNR values will be given in specific tests.

For the periodic sensing model, we set the parameters similarly to the requirement in IEEE WRAN 802.22. The value of T_s is fixed, while the length of T_p can be changed, and sensing scheduling is applied to choose an appropriate discrete T_p. In 802.22 WRAN, T_p may only take values that are multiples of a MAC frame size 10 ms due to many higher-layer concerns such as synchronization. Specifically, we set the sensing block duration $T_s = 20\ \mu$s, with the channel detection time $CDT = 40$ms and the required $P_{FA} = P_{MD} = 0.01$. Rather than using the Nyquist sampling rate $f_{nyq} = 1$ GHz, we adopt the sub-Nyquist sampling rate $f_{sub} = 0.25$ GHz. The number of compressed samples in a sensing block T_s is $M = f_{sub}T_s = 5{,}000$, whereas the Nyquist number $N = f_{nyq}T_s = 20{,}000$. An example of the wideband signal spectrum, noisy spectrum and recovered spectrum using CS is presented in Fig. 6, where the SNR is -5 dB. The wideband signal has three 10 MHz sub-bands occupied with the center frequencies of 75, 125 and 225 MHz respectively.

We also set the MAC frame size $FS = 200\ \mu$s. Table 1 lists some default normalized T_p values (with respect to the MAC frame size FS) under a range of SNR levels as determined by Eqs. (26) and (27).

7.2 Performance and Analysis

7.2.1 Change Detection and In-Depth Sensing Action

A list of change detection thresholds and in-depth sensing action is given in Table 2. From the table, we can see the schemes differ by the factor δ, which controls the sensitivity of a SU to the change of the sampled group of data in order to trigger the in-depth sensing. Scheme "sched1-4' does not perform the in-depth sensing. In the schemes "sched1-1" to "sched1-3", the change threshold factor δ in Eq. (25) is kept the same and the T_p adjustments are different in the in-depth sensing, while in schemes "sched2-1" to "sched2-3", δ is different and T_p adjustment is set the same. Note that all the listed schemes are in the model of moving-CDT, backward GCD-SPRT, and if in-depth sensing is triggered, no decision will be made till next original T_p. In-depth sensing period T_p^{elev} is immediately reduced to a certain pre-determined value, but no decision is made until the original scheduled T_p time is reached; in other words, the in-depth sensing serves to provide more data.

TABLE 2
In-Depth Sensing Scheduling

notation	explanation
"sched1-1"	$\delta = 2, T_p^{elev} \leftarrow 2FS$
"sched1-2"	$\delta = 2, T_p^{elev} \leftarrow 3FS$
"sched1-3"	$\delta = 2, T_p^{elev} \leftarrow 4FS$
"sched1-4"	w/o change detection or in-depth sensing
"sched2-1"	$\delta = 1, T_p^{elev} \leftarrow 2FS$
"sched2-2"	$\delta = 2, T_p^{elev} \leftarrow 2FS$
"sched2-3"	$\delta = 3, T_p^{elev} \leftarrow 2FS$
"sched2-4"	w/o change detection or in-depth sensing

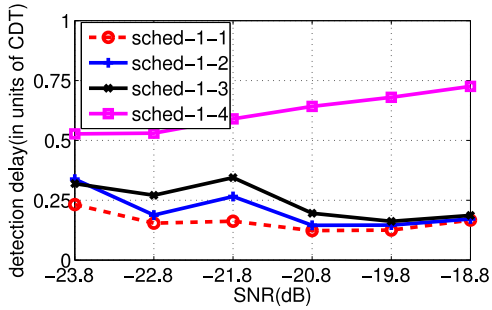

Fig. 7. Effects of in-depth sensing on decision delay.

In Figs. 7 and 8, the effects of different in-depth scheduling with SWCS are investigated. Two metrics are used to analyze the effectiveness of sensing scheduling: decision delay, defined as the average time taken to make the final decision on PU's presence after its return, and probability of decision failure, the probability that the PU's presence is still not detected when the CDT time limit has reached since the appearance of PU. As expected, both metrics decrease as T_p is reduced to accelerate the sequential sensing process and gather more data for faster decision. Our proposed scheme "sched1-1" greatly outperforms the "sched1-4" (GCD-SPRT without in-depth sensing for change detection), by more than 50 and 90 percent in terms of the detection delay and probability of failure, respectively. This indicates that scheduling change detection and in-depth sensing are beneficial since the extra sensing effort is likely to expedite the decision making by more quickly leading the sequential test out of the intermediate zone between the thresholds A and B.

In Figs. 9 and 10, the effects of different thresholds for triggering in-depth sensing with SWCS are investigated. The trend in detection failure probability is the same as that in the average detection delay. As the average delay goes up, the PU will have a smaller chance to be detected by the CDT deadline. As the threshold factor δ increases, the decision delay and probability of detection failure get worse. The smaller δ is, the easier it is for the SU to quickly trigger in-depth sensing. We observe that the scheme with default

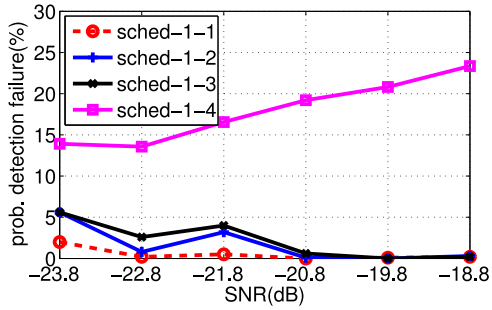

Fig. 8. Effects of in-depth sensing on decision failure.

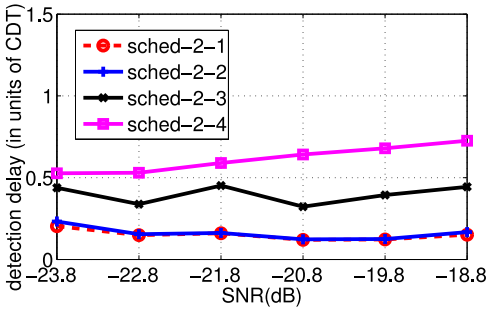

Fig. 9. Effects of change detection on decision delay.

parameters "sched2-2" ($\delta = 2$) greatly outperforms the baseline scheme without change detection and in-depth sensing "sched2-4". Note that when δ goes to infinity, it is equivalent to the cases where in-depth sensing actions will never be triggered. Interestingly, we observe that the performance degrades somewhat as SNR increases. With a higher SNR, the default initial T_p is larger (see Table 1) which introduces a higher initial delay before an SU responds by triggering the in-depth sensing, which also affects the probability of decision failure.

7.2.2 Spectrum Analysis and Fusion

For schemes except SWCS-BS, we use ℓ_1-magic as our reconstruction algorithm [28], although some other modified reconstruction algorithm can also be used, such as some greedy algorithms proposed in [34]. For SWCS-BS, we exploit the proposed block-sparse CS recovery algorithm to reconstruct the wideband power spectrum.

To assess the effects of different fusion schemes that merge the CS-recovered spectrum from each sensing time block T_s, we evaluate in SWCS framework the performances of different fusion schemes under $SNR = -5$ dB in Fig. 11. The false alarm/missed detection ratio is defined as the number of false-alarmed/miss-detected sub-bands divided by the number of actually occupied sub-bands. With the simple OR rule, large noise effects result in high false alarm ratios, as a sub-band is considered to be occupied as long as the sub-band is estimated to be occupied in any sensing period. The false estimation in a period may be caused by an abrupt noise. Nevertheless, the missed detection ratio is very low. The AND rule also cannot handle the abrupt fluctuations well, and it has high missed detection ratio because it only regards the sub-band to be occupied when the sub-band is estimated to be occupied in all the sensing periods, although this can result in a small false alarm ratio. The

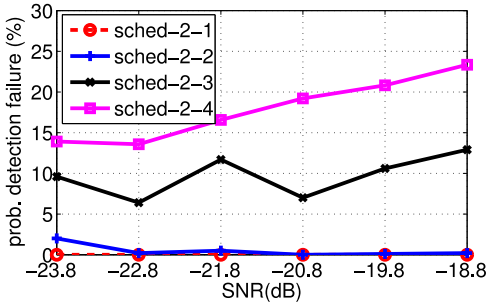

Fig. 10. Effects of change detection on decision failure.

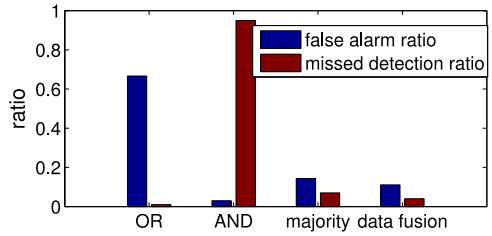

Fig. 11. Different spectrum fusion schemes.

majority decision fusion (a sub-band is finally identified as occupied if more than half of the spectrum maps collected indicate so) and data fusion perform better in balancing the false alarm ratio and missed detection, because these two deal with the wrong sub-band status more softly in the merging process. The majority decision fusion is slightly worse than the data fusion which fuses the spectrum energy values, rather than 0/1 decisions, in each map.

7.2.3 SWCS Peer Schemes

A list of peer algorithms along with the proposed SWCS is shown in Table 3. The peer schemes may differ in one or more aspects from the proposed SWCS and SWCS-BS. We compare these peer schemes using the following metrics: sampling overhead, recovery overhead and probability of decision failure. *Sampling overhead* is defined as the ratio of total number of actual samples (may be sub-Nyquist, Nyquist or both) over the total number of samples required by Nyquist sampling theorem. *Recovery overhead* is defined as the number of T_p periods to incur CS recovery over the total number of T_p periods. *Decision delay* is defined as the average time overhead used to make final decision of PU's presence after its return. As there are no existing schemes studying the continuous sensing over wide spectrum band, we compare the performance of our work with three peer schemes: "sequential w/o CS", "periodic CS" and "sequential with CS". We set $SNR = -18.8$ dB in Fig. 12, where the decision delay is normalized as the ratio of the actual delay of each to the maximum of the four.

The scheme without CS has a high overhead due to the Nyquist sampling, although it has no CS recovery overhead. The detection delay of our proposed SWCS is comparable to that of *sequential without CS* but with more than 60 percent less sampling overhead. SWCS also has at least 50 percent lower recovery overhead compared to various CS-based schemes, as its only performs recovery when certain conditions are met. The *periodic CS* scheme has a small sampling overhead but performs worse than others in terms of the decision delay because it lacks scheduled sequential

TABLE 3
SWCS and SWCS-BS Peer Schemes Comparison

notation	explanation
"SWCS","SWCS-BS"	default $\delta = 2$, $T_p^{elev} \leftarrow 2FS$
"sequential w/o CS"	SWCS without CS/with Nyquist sampling
"periodic CS"	periodic detection w/o sequential analysis
"sequential with CS"	SWCS with always-recovery in GCD-SPRT

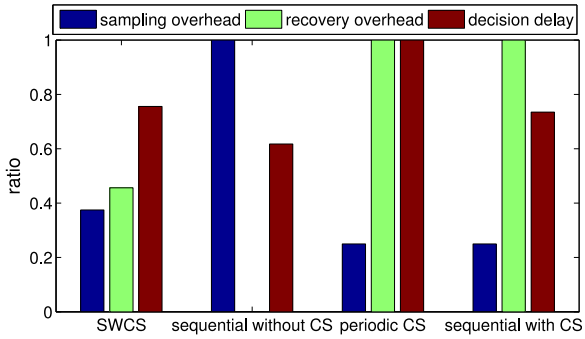

Fig. 12. Comparison of peer schemes.

detection that helps speed up the decision process. The *sequential with CS* scheme performs slightly better than SWCS in terms of the sampling overhead and decision delay but has large recovery overhead. To conclude, our SWCS can achieve a satisfactory trade-off between sampling overhead, recovery overhead, and decision delay.

7.2.4 Block-Sparse Recovery (SWCS-BS)

We have evaluated the advantages of our proposed SWCS. Now we will assess SWCS-BS. Recall that the difference between our proposed SWCS and SWCS-BS is the latter exploits the block-sparse properties of the wideband. The performances of SWCS (sched-1-1), SWCS-BS and a baseline scheme (sched-1-4) are depicted in Figs. 13 and 14.

In Fig. 13, in terms of the detection delay, SWCS-BS is able to obtain a maximum of 40 percent improvement compared to SWCS (at $SNR = -18.8$ dB). Compared to SWCS, SWCS-BS exploits the block-sparse characteristics of wideband power spectrum to improve the reconstruction accuracy under given measurements, thus enabling the SU to detect possible PU activities more rapidly and precisely.

Since the accuracy of detection is significantly impacted by CS reconstruction, SWCS-BS is expected to outperform SWCS and achieve a smaller detection failure probability. As validated in Fig. 14, SWCS-BS can achieve an improvement as large as 50 percent (when $SNR = -18.8$ dB) compared to SWCS in terms of detection failure.

Figs. 13 and 14 indicate that exploiting the block features of wideband power spectrum can significantly improve the CS reconstruction performances and thus make the sequential sensing of the wideband more efficient. We can see the improvement becomes larger as SNR reduces initially. But when the SNR values are too low, due to the lack of clear block structure, the performance improvement of SWCS-BS becomes smaller.

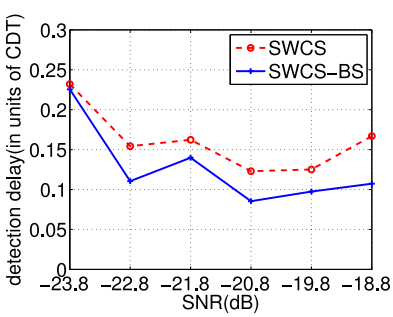

Fig. 13. Effects of block sparsity on detection delay.

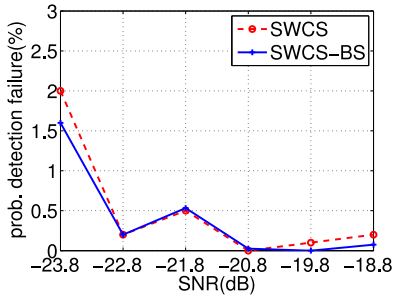

Fig. 14. Effects of block sparsity on detection failure.

Our proposed SWCS-BS presents its effectiveness in many folds: it not only benefits from the low-cost sequential wideband compressed sensing (SWCS) framework, but also further takes advantage of the proposed block-sparse CS reconstruction algorithm to improve the sensing performance.

8 Conclusion

This paper presents two integrated frameworks (SWCS and SWCS-BS) to efficiently schedule sequential periodic wideband sensing based on sub-sampled data, where the compressed sensing technique is incorporated into the sequential detection to ensure low overhead and more accurate wideband sensing. Backward grouped-compressed-data sequential probability ratio test (backward GCD-SPRT) is introduced for sequential detection to reduce the decision delay. In addition, we propose an algorithm to find potential H_0-to-H_1 change, after which in-depth sensing is scheduled to accelerate sensing decisions and improve the accuracy. We also propose to exploit the block sparsity of the wideband power spectrum to improve the CS reconstruction quality thus the sensing performance. Finally, we study a set of schemes to fuse spectrum signals recovered from sparse samples in spectrum analysis for more accurate spectrum usage detection. Simulation results demonstrate the significant advantages of our design in reducing the sensing delay, detection failure, as well as sampling and CS recovery overhead.

Acknowledgments

Xin Wang's research has been supported by the US National Science Foundation under grant ECCS-1408247 and Shiwen Mao's research has been supported by the US National Science Foundation under grants CNS-1247955 and CNS-1320664.

References

[1] S. Haykin, "Cognitive radio: Brain-empowered wireless communications," *IEEE J. Sel. Areas Commun.*, vol. 23, no. 2, pp. 201–220, Feb. 2005.
[2] Q. Zhao and B. M. Sadler, "A survey of dynamic spectrum access," *IEEE Signal Process. Mag.*, vol. 24, no. 3, pp. 79–89, May 2007.
[3] D. L. Donoho, "Compressed sensing," *IEEE Trans. Inf. Theory*, vol. 52, no. 4, pp. 1289–1306, Apr. 2006.
[4] E. J. Candès, "Compressive sampling," presented at the *Int. Congr. Mathematicians*, Madrid, Spain, 2006.
[5] Z. Tian and G. B. Giannakis, "Compressed sensing for wideband cognitive radios," in *Proc. IEEE Int. Conf. Acoust. Speech Signal Process.*, 2007, pp. IV-1357–IV-1360.
[6] H. Sun, W. Y. Chiu, and A. Nallanathan, "Adaptive compressive spectrum sensing for wideband cognitive radios," *IEEE Commun. Lett.*, vol. 16, no. 11, pp. 1812–1815, Nov. 2012.

[7] Q. Liu, X. Wang, and Y. Cui, "Scheduling of sequential periodic sensing for cognitive radios," in *Proc. IEEE INFOCOM*, Apr. 2013, pp. 2256–2264.
[8] Q. Liu, X. Wang, and Y. Cui, "Robust and adaptive scheduling of sequential periodic sensing for cognitive radios," *IEEE J. Sel. Areas Commun.*, vol. 32, no. 3, pp. 503–515, Mar. 2014.
[9] A. Wald, *Sequential Analysis*. New York, NY, USA: Wiley, 1947.
[10] H. Kim and K. G. Shin, "In-band spectrum sensing in cognitive radio networks: Energy detection or feature detection?" in *Proc. 14th ACM Int. Conf. Mobile Comput. Netw.*, 2008, pp. 14–25.
[11] A. W. Min and K. G. Shin, "An optimal sensing framework based on spatial RSS-profile in cognitive radio networks," in *Proc. 6th Annu. IEEE Commun. Soc. Conf. Sensor Mesh Ad Hoc Commun. Netw.*, Jun. 2009, pp. 1–9.
[12] J. Guo, G. Zhong, D. Qu, and T. Jiang, "Multi-slot spectrum sensing with backward SPRT in cognitive radio networks," in *Proc. Int. Conf. Wireless Commun. Signal Process.*, 2010, pp. 1–5.
[13] A. K. Jayaprakasam and V. Sharma, "Cooperative robust sequential detection algorithms for spectrum sensing in cognitive radio," in *Proc. Int. Conf. Ultra Modern Telecommun. Workshops*, Oct. 2009, pp. 1–8.
[14] H. Li, C. Li, and H. Dai, "Quickest spectrum sensing in cognitive radio," in *Proc. 42nd Annu. Conf. Inf. Sci. Syst.*, Mar. 2008, pp. 203–208.
[15] Z. Quan, S. Cui, A. H. Sayed, and H. V. Poor, "Optimal multiband joint detection for spectrum sensing in cognitive radio networks," *IEEE Trans. Signal Process.*, vol. 57, no. 3, pp. 1128–1140, Mar. 2009.
[16] Y. L. Polo, Y. Wang, A. Pandharipande, and G. Leus, "Compressive wide-band spectrum sensing," in *Proc. IEEE Int. Conf. Acoust. Speech Signal Process.*, 2009, pp. 2337–2340.
[17] Y. Wang, Z. Tian, and C. Feng, "A two-step compressed spectrum sensing scheme for wideband cognitive radios," in *Proc. IEEE Global Telecommun. Conf.*, Dec. 2010, pp. 1–5.
[18] Z. Tian, Y. Tafesse, and B. M. Sadler, "Cyclic feature detection withsub-Nyquist sampling for wideband spectrum sensing," *IEEE J. Sel. Topics Signal Process.*, vol. 6, no. 1, pp. 58–69, Feb. 2012.
[19] Z. Qin, Y. Gao, and C. G. Parini, "Data-assisted low complexity compressive spectrum sensing on real-time signals under sub-Nyquist rate," *IEEE Trans. Wireless Commun.*, vol. 15, no. 2, pp. 1174–1185, Feb. 2016.
[20] Z. Qin, Y. Gao, M. D. Plumbley, and C. G. Parini, "Wideband spectrum sensing on real-time signals at sub-Nyquist sampling rates in single and cooperative multiple nodes," *IEEE Trans. Signal Process.*, vol. 64, no. 12, pp. 3106–3117, Jun. 2016.
[21] D. Romero, D. D. Ariananda, Z. Tian, and G. Leus, "Compressive covariance sensing: Structure-based compressive sensing beyond sparsity," *IEEE Signal Process. Mag.*, vol. 33, no. 1, pp. 78–93, Jan. 2016.
[22] H. Zhang, Z. Zhang, and Y. Chau, "Distributed compressed wideband sensing in cognitive radio sensor networks," in *Proc. IEEE Conf. Comput. Commun. Workshops*, 2011, pp. 13–17.
[23] F. Zeng, C. Li, and Z. Tian, "Distributed compressive spectrum sensing in cooperative multihop cognitive networks," *IEEE J. Sel. Topics Signal Process.*, vol. 5, no. 1, pp. 37–48, Feb. 2011.
[24] Y. Ma, Y. Gao, Y. C. Liang, and S. Cui, "Reliable and efficient sub-Nyquist wideband spectrum sensing in cooperative cognitive radio networks," *IEEE J. Sel. Areas Commun.*, vol. 34, no. 10, pp. 2750–2762, Oct. 2016.
[25] M. Derakhtian, F. Izedi, A. Sheikhi, and M. Neinavaie, "Cooperative wideband spectrum sensing for cognitive radio networks in fading channels," *IET Signal Process.*, vol. 6, no. 3, pp. 227–238, 2012.
[26] S. Srinu and S. L. Sabat, "Cooperative wideband sensing based on entropy and cyclic features under noise uncertainty," *IET Signal Process.*, vol. 7, pp. 655–663, Oct. 2013.
[27] J. Zhao, X. Wang, and Q. Liu, "Cooperative sequential compressed spectrum sensing over wide spectrum band," in *Proc. IEEE Int. Conf. Sensing Commun. Netw.*, Jun. 2015, pp. 1–9.
[28] E. J. Candès and J. Romberg, "ℓ_1 -magic: Recovery of sparse signals via convex programming," 2005, https://scholar.google.com/scholar?cluster=15275895701574443820&hl=en&as_sdt=5,33&sciodt=0,33
[29] D. Needell and J. Tropp, "CoSaMP: Iterative signal recovery from incomplete and inaccurate samples," *Appl. Comput. Harmonic Anal.*, vol. 26, no. 3, pp. 301–321, May 2009.
[30] M. Stojnic, F. Parvaresh, and B. Hassibi, "On the reconstruction of block-sparse signals with an optimal number of measurements," *IEEE Trans. Signal Process.*, vol. 57, no. 8, pp. 3075–3085, Aug. 2009.
[31] J. Zhao and X. Wang, "Channel sensing order for multi-user cognitive radio networks," in *Proc. IEEE Int. Symp. Dyn. Spectrum Access Netw.*, Oct. 2012, pp. 397–407.
[32] Z. M. Charbiwala, et al., "Compressive oversampling for robust data transmission in sensor networks," in *Proc. IEEE INFOCOM*, 2010, pp. 1–9.
[33] Z. Weng and X. Wang, "Support recovery in compressive sensing for estimation of direction-of-arrival," in *Proc. Conf. Rec. 45th Asilomar Conf. Signals Syst. Comput.*, 2011, pp. 1491–1495.
[34] J. Zhao and X. Wang, "Compressive wireless data transmissions under channel perturbation," in *Proc. IEEE Int. Conf. Sensing Commun. Netw.*, Jun. 2014, pp. 212–220.

Jie Zhao received the BS degree in telecommunications engineering from the Huazhong University of Science and Technology, Wuhan, China. Currently, he is working toward the PhD degree in the Department of Electrical and Computer Engineering, State University of New York at Stony Brook, New York. His current research interests include compressed sensing, cognitive radio networks, networked sensing, and detection as well as millimeter-wave communications. He is a student member of the IEEE.

Qiang Liu received the PhD degree in electrical and computer engineering from Stony Brook University, Stony Brook, New York, in 2014. He is currently a research associate in the Computational Sciences and Engineering Division, Oak Ridge National Laboratory, Oak Ridge, Tennessee. His research areas include networked data and information fusion, signal/target detection and estimation, statistical signal processing, wireless sensor networks, cognitive radios, cyber-physical systems, transport protocols, high performance computing, and software defined networking. He has published more than 25 peer-reviewed papers in prestigious conference proceedings and journals, and has reviewed dozens of works by others. He has been invited to present his work at various venues and has received several best paper and travel grant awards. He is a member of the IEEE.

Xin Wang received the BS and MS degrees in telecommunications engineering and wireless communications engineering, respectively, from the Beijing University of Posts and Telecommunications, Beijing, China, and the PhD degree in electrical and computer engineering from Columbia University, New York. She is currently an associate professor in the Department of Electrical and Computer Engineering, State University of New York at Stony Brook, Stony Brook, New York. Before joining Stony Brook, she was a member of technical staff in the area of mobile and wireless networking at Bell Labs Research, Lucent Technologies, New Jersey, and an assistant professor in the Department of Computer Science and Engineering, State University of New York at Buffalo, Buffalo, New York. Her research interests include algorithm and protocol design in wireless networks and communications, mobile and distributed computing, as well as networked sensing and detection. She has served on executive committees and technical committees of numerous conferences and funding review panels, and serves as the associate editor of the *IEEE Transactions on Mobile Computing*. She achieved the NSF Career Award in 2005, and ONR Challenge Award in 2010. She is a member of the IEEE.

Shiwen Mao received the PhD degree in electrical and computer engineering from Polytechnic University, Brooklyn, New York (now Tandon School of Engineering of New York University, New York), in 2004. Currently, he is the Samuel Ginn distinguished professor and director of the Wireless Engineering Research and Education Center, Auburn University, Auburn, Alabama. His research interests include wireless networks, multimedia communications, and smart grid. He is a distinguished lecturer of the IEEE Vehicular Technology Society. He is on the editorial boards of the *IEEE Transactions on Multimedia*, the *IEEE Internet of Things Journal*, the *IEEE Multimedia*, the *ACM GetMobile*, among others. He is the chair of the IEEE ComSoc Multimedia Communications Technical Committee. He received the NSF CAREER Award in 2010. He is a co-recipient of the Best Demo Award from IEEE SECON 2017, the Best Paper Awards from IEEE GLOBECOM 2016, IEEE GLOBECOM 2015, IEEE WCNC 2015, and IEEE ICC 2013, and the 2004 IEEE Communications Society Leonard G. Abraham Prize in the Field of Communications Systems. He is a senior member of the IEEE.